УДК. 539.21:544.03:546.2

Т.С. ТУРМАГАМБЕТОВ, Х.А. АБДУЛЛИН,
Б.Н. МУКАШЕВ, А.К. АХМЕТОВ И М.М. АХМЕТОВ

ИССЛЕДОВАНИЕ ПРОФИЛЯ РАСПРЕДЕЛЕНИЯ И КИНЕТИКИ ФОРМИРОВАНИЯ ТЕРМОДОНОРОВ В КРЕМНИИ

Исследованы образцы монокристаллического кремния n-Cz-Si, выращенного методом Чохральского. Тонкий легированный слой на поверхности образцов создавался быстрой диффузией бора, алюминия, фосфора либо олова из поверхностного источника при температуре ~1000°С в течение 10 секунд. Термодоноры (ТД) формировались при отжиге 450°С в течение времени от 3 до 384 часов на воздухе. Профили концентрации заряженных центров определялись при обработке измеренных вольт-фарадных характеристик. Обнаружено, что в образцах с поверхностным слоем, легированным бором либо алюминием, вблизи поверхности концентрация ТД существенно ниже, чем в контрольных образцах и образцах, легированных фосфором или бором, и сравнивается с объемной концентрацией только на глубинах от 2 до 15 микрон в зависимости от времени отжига при 450°С. Эффект неоднородного распределения ТД не связан с обеднением приповерхностных слоев кислородом и может быть объяснен уменьшением концентрации собственных междоузельных атомов, выступающих катализаторами процесса формирования ТД. При этом приповерхностные слои, легированные бором или алюминием, играют роль эффективных стоков для междоузельных атомов.

Введение

Монокристаллический кремний является основным материалом полупроводниковой электроники. Его получают из поликристаллического кремния двумя основными способами: методом зонной очистки и методом вытягивания из расплава. В методе зонной очистки получается высокочистый кремний (FZ-Si) с низким содержанием кислорода (~10^{15}-5×10^{16} $см^{-3}$) и других примесей, однако максимальный диаметр получающегося монокристалла ограничивается величиной ~75 мм. Метод вытягивания из расплава позволяет получать монокристаллы кремния (Cz-Si) большого диаметра (вплоть до 300 мм), что повышает экономическую эффективность производства. Расплавленный кремний обладает высокой растворяющей способностью, в результате взаимодействия с материалом кварцевого тигля

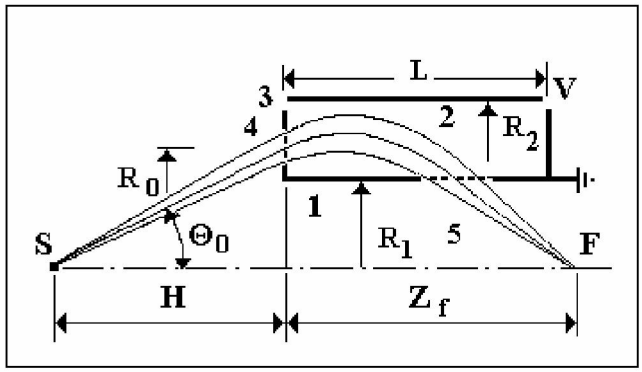

Fig.1. The schematic cross-section view of the upper part the focusing system.
1- the inner cylinder , 2- the outer cylinder , 3- the boundary electrode with the entrance window (4),
5- the exit window, S- a charged particles source, F- the point focus

is very different from well known cylindrical mirror field.

Calculations

The field used is a solution of the Laplace equation $\nabla^2 U(R,Z) = 0$ with boundary conditions: $U(R_1, Z) = U(R, 0) = U(R, L) = 0$, $U(R_2, Z) = V$ and restricted by concentric cylindrical surfaces and two boundaries along Z-axis (see scheme in Fig.1).

The potential distribution can be written as follows:

$$U(r.z) = \frac{4V}{\pi} \cdot \sum_{m}^{\infty} \sin(2m+1)\frac{\pi z}{l} \cdot \frac{F_m(r)}{F_m(\beta)(2m+1)} \quad (1)$$

The lengths in (1) and below were scaled with R_1 in order of introducing the dimensionless parameters: $r=R/R_1$, $z=Z/R_1$, $l= L/R_1$, $\beta=R_2/R_1$, $r_0=R_0/R_1$, $h=H/R_1$. Here $F_m(r) = (I_0(k_m r)K_0(k_m)-I_0(k_m)K_0(k_m r)) / K_0(k_m)$, $k= (2m+1)\pi_m / l$. I_0 and K_0 – are modified Bessel and Hankel functions respectively. The central part of this field, displayed the potential distribution the same as that in a cylindrical mirror field when l is much greater than β - 1:

$$\ddot{z} = -\frac{e}{m} U(r,z) \frac{\ln(r)}{\ln(\beta)} \partial z \quad (2)$$

The non-relativistic equations of motion in the general field (1) are given by:

$$\ddot{r} = -\frac{e}{m} \partial U(r,z) / \partial r \quad (3)$$

$$\ddot{z} = -\frac{e}{m} \partial U(r,z) / \partial z \quad (4)$$

The system of equations (3), (4) has been integrated numerically to determine the trajectories of charged particles of a single kinetic energy entering into the cylindrical field within the beam with central trajectory angle equal θ_0.

It should be noticed that there are two main points, relating to accuracy of calculations in general. Firstly, we investigated the effect of addends number involved by calculation of the sum in (1). Direct calculations of the sum in the right-handed members in (3) and (4) were made to N = 90 addends. Checking was made by comparison of the length Z_f for trajectories with the sum upper limits N and N+10. If $abs((Z_f)_{N+10} - (Z_f)_N) \le 0.001$ was achieved the value N was used. Secondly, it was also important to find out the optimal criterion for precision of numerical calculations of trajectory coordinates. In order to establish the optimal value of calculation time step we performed a comparison of calculations with the results of analytical calculations in our paper [3] for cylindrical mirror field with first order focusing for a parallel flow. When simulating the cylindrical mirror field, value l = 31 was taken and particles were started at z = 14. In this case the trajectories locate entirely in the region of field given by (2). Calculations were performed using Runge-Kutta method , with absolute accuracy of the final coordinate about 0.002. For the case of the field (1) for particles entering at the entrance window (see Fig.1) potential distribution (2) was found existing near the exit window when calculation has been performed by l = 31. Later it was established that logarithmic field (2) near the exit window kept non-distort until l was several times large than β -1.

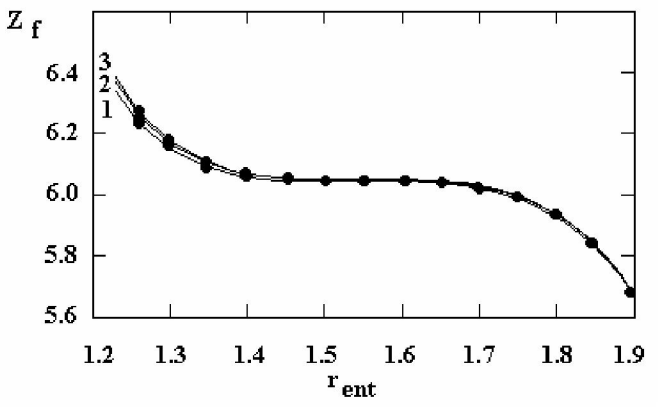

Fig.2. The illustration of refocusing ability
of the system in to different point by a constant value of z_f for some set of parameters.
1-S=60, E_0/eV = 4.86 ; 2- S= 80, E_0/eV = 4.95; 3- S=100, E_0/eV = 5.0

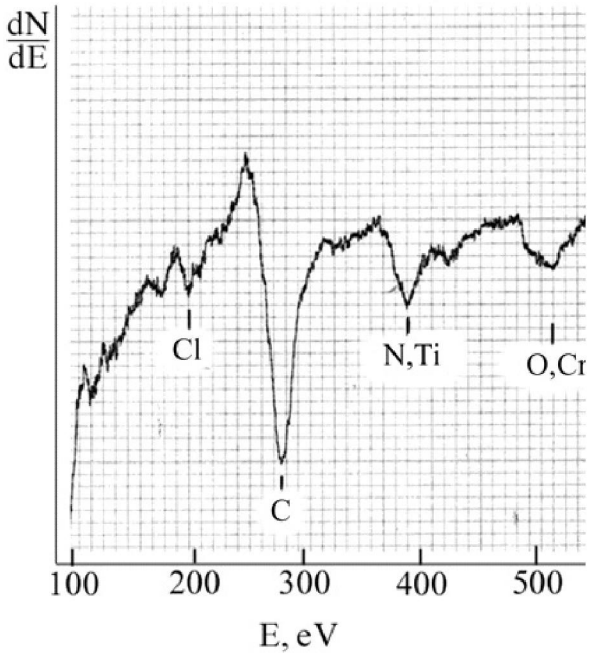

Fig.3. The typical Auger spectrum obtained from a distant surface

Regressions (5), (6) were obtained from numerical calculations in order to predict effect of increasing β value on the main focussing parameters in the case of parallel flow for configuration with l = 31. Value of β was ranged in interval 1.8 – 3.0.

$$Z_f = 3.665 + 2.903\beta - 0.775\,\beta^2 \qquad (5)$$

$$G = 23.54 - 12.389\beta + 1.756\,\beta^2 \qquad (6)$$

The regressions above relate to the central trajectory parameters. Increasing the β value allows to obtain the higher transmission but in that case it is necessary to use larger values of l, in order to avoid the disturbing effect of the right-side end-plate. Calculations were also performed for lower value of l in order to find out conditions for designing a practical compact device without any end-field correction system. For example, a compact shorten analyzer without any fringe field correction system can be made with l = 5.5 in the case h = 8, G = E_0/eV = 3, with focusing length equal to 5.43. It was established that by β lower 2.3 aberration figure shape displayed a second order focussing for this shorten configuration without disturbing effect of the right-side boundary.

When combining the large β with short length it is necessary to use an end-field correction system behind the exit window (it corresponds to calculation with l =31).

The system presented provides very useful property - a distant h to source can be changed by negligible variations of focussing characteristics by the same value of z_f, which is commonly a parameter of device, (Fig.2).

Corresponding values of G can be calculated for the new h values in order to save the second order focusing by a constant z_f.

The energy resolution ability defined as $D / \Delta z_f$, where Δz_f ,as known very well, is a projection of the part of aberration figure around a central point on the z_f-z_0 axis.

The dispersion $D = (\partial z_f / \partial E) \cdot E$ for this system was estimated numerically on average as large as $D = 4.0$.

Fig.3 presents the Auger – spectrum obtained in testing experiments from the distant specimen. The distance between the entrance window-plate of the analyzer and the distant target point was equal nearly 16 cm.

Conclusion

The focusing characteristics of a cylindrical field limited along the symmetry axis have been numerically investigated for the case of a distant source of charged particles. It was found out that this configuration of a cylindrical field bounded provides the second order focusing. The system presented has been used for production the electron energy prototype-analyzer with compact and simple design , very suitable for experimental treatment.

REFERENCES

1. *Palmberg P.W., Bohn G.R., Tracy J.C.* // Appl.Phys.Lett.1969. 15. 254

2. *Ilyin A. M.* // J. Electron Spectrosc. and Relat. Phenom. 2001. 120. 89

3. *Ilyin A. M. and Borisov B. A.* // Measur. Sci. Technol.2001. 12. 2015

4. *Ilyin A. M.* // Nucl. Instrum.Methods Phys.Res. 2003. A 500. 62.

5. *Ilyin A.M. and Ilyina I.A.*// Measur. Sci. Technol.2005. 16. 1798.

Резюме

Жұмыста жарық жылдамдығынан біршама аз қозғалатын зақымданған бөліктер (нерелятивтік бөлшектер) үшін цилиндрлік өрістің екі шекарасының фокусталған қасиеттерінің теориялық зерттеулерінің нәтижелері көрсетілген. Шығаратын бөлшектердің көзі талдауыштан (анализатор) біршама қашық, симметрия осінде орналасқан. Екінші дәрежелі фокустелудің бірнеше жағдайлары табылған. Фокусировка параметрлерінің вариациясы зерттелген және біршама регрессивтік қатынастар алынған. Осы теориялық қорытындылардың негізінде анализатордың тәжірибелік үлгісі құрылған. Қашықтағы жазықтықтан эксперименталды оже-спектрлар алынған.

Резюме

В работе представлены результаты теоретических исследований фокусирующих свойств цилиндрического поля с двумя границами, расположенными вдоль оси симметрии для заряженных частиц, двигающихся много меньше скорости света (нерелятивистских частиц). Источник испускаемых частиц находился вдали от анализатора, на оси симметрии. Были найдены некоторые условия фокусировки второго порядка. Были изучены вариации параметров фокусировки и получены некоторые регрессионные соотношения. На основе этих теоретических выводов был построен опытный образец-анализатор. Получены экспериментальные оже-спектры от удаленной поверхности.

НИИ ЭТФ КазНУ,
г. Алматы

Поступила 19.10.09 г.